PORT SAID ENGINEERING RESEARCH JOURNAL

Faculty of Engineering - Port Said University
Volume 26 No. 4 pp: 50-55

# Hybrid Central Composite Design and Genetic Algorithm to Optimize Turning Parameters for Surface Roughness in Self-propelled Rotary Tools

*H. Kouta*[1], *S. Elsanabary*[1,*]

[1] *Department of Production Engineering and Mechanical Design, Faculty of Engineering, Port Said University, Port Said, 42523, Egypt, email: Hanan.kamel@eng.psu.edu.eg*

* *S. Elsanabary,Email, Samar.abaas@eng.psu.edu.eg , DOI: 10.21608/pserj.2022.154750.1191*

*Received 7-8-2022,*
*Revised 30-8-2022,*
*Accepted 4-9-2022*

*© 2022 by Author(s) and PSERJ.*

*This is an open access article licensed under the terms of the Creative Commons Attribution International License (CC BY 4.0).*
*http://creativecommons.org/licenses/by/4.0/*

## ABSTRACT

This paper investigates experimentally the efficiency of a self-propelled rotary tool (SPRT) using carbide inserts during turning of K110 alloy steel. The cutting conditions, namely, cutting velocity $v_c$ (m/min), feed rate f (mm/rev), and depth of cut $a_p$ (mm) were interacted at a constant tilting angle of 20°, while considering the surface roughness ($R_a$) as performance criteria. The exploratory strategy is based on the central composite design (CCD), which was used to investigate at the influence of cutting boundaries on a superficial harshness level to observe the optimal cutting conditions. A second-order regression model was created. The performance parameters of the turning operation were studied using analysis of variance. A genetic algorithm (GA) was applied to optimize the SPRT cutting condition. The surface roughness and corresponding cutting conditions were optimized by creating a hybrid CCD-GA. The results showed that vc has the most impact on $R_a$, followed by f and $a_p$. The minimum $R_a$ value was 0.58 µm obtained at 140 m/min of $v_c$, 0.04 mm/rev off, and 0.3 mm of $a_p$. Finally, GA and hybrid CCD-GA optimization techniques have optimal surface roughness and compared with experimental results.

**Keywords**: Self-propelled rotary tool, Surface roughness, Optimization, Hybrid CCD-GA

## 1 INTRODUCTION

Hard-to-cut materials including nickel-based alloys, titanium, and toughened steel are currently used in the biomedical, aerospace, and automotive industries. High-thermal strength, wear resistance, and chemical stability are characteristics of hard-to-cut materials. These materials are challenging to a machine due to extreme wear and high heat concentrations created during the process [1] [2]. Excessive cutting tool wear is a major problem in conventional turning using a single-point cutting tool when machining difficult-to-cut materials. Tool wear causes poor surface finish on machined parts and increases production time and cost due to stoppages to change inserts [3]. To improve tool life, researchers have focused on issues related to cutting tool wear resistance, such as the influence of tool coatings and cutting parameters [4] [5].

For turning brittle materials, a rotary tool can be used instead of a single-point insert, continuously presenting a new tool edge into the machining zone for tool life recovery and surface quality improvement by eliminating the effect of high temperatures and thermal energy generated in the cutting zone [3]. A rotary tool uses a round cutting insert revolving around its primary axis. Rotary tools are divided into self-propelled (SPRT) and actively driven (ADRT). The cutting edge inclination angle relating to the workpiece generates the SPRT process, whereas the ADRT process necessitates using an external motor to control the insert rotational speed [6]–[8].

At the beginning of the 21st century, Kishawy et al. [9] used the work–tool geometric interaction and empirical function to simulate the behavior of flank wear for SPRTs. The authors conducted an experimental cutting on AISI4340 steel under various cutting conditions. They discovered that the feed rate has a comparable impact on flank wear of SPRT development in hard turning, as the cutting speed range is 139–446 m/min. The efficiency of the proposed model was also demonstrated by a strong connection between simulated

and observed flank wear. Kossakowska et al. [10] examined applying SPRT for turning high alloy steel 15H11MF. The authors investigated the impact of chip development on the created surface. In the milling process, Suzuki et al. [11] provided a model for estimating the cutting force and movement of the revolving insert in SPRT operations. The experiment was conducted on brass under cutting conditions. According to the authors, the suggested model precisely anticipated the cutting forces and rotation motions.

A multifunctional statistical tool called Response Surface Methodology (RSM) uses an evidence-based set of mathematics and statistical methods to build, improve, and optimize processes. Based on their individual and interactive impacts, RSM connects responses efficiency's real and modeled behavior to various effective parameters. For modelling and empirical optimization in RSM, Central Composite Design (CCD) is utilized. [12].

Many studies have optimized the SPRT cutting condition using GA. Rao et al. [13] investigated the cutting performance of SPRT, including surface finish and metal removal rate (MRR), while turning hardened EN24 steel. The cutting conditions, including the spindle speed, SPRT inclination angle, feed rate, and, depth of cut was optimized using the nondominated sorting genetic algorithm-II (NSGA-II). The resulting optimum solution correlated well with the experimental ones. Baki et al. [14] applied an integrated multi-objective optimization approach of the SPRT process for machine hardened EN24 (SAE4340) steel. Under various cutting parameters, the surface finish, and MRR were measured as evaluation criteria. The authors integrated gray rotational analysis (GRA), RSM, and GA to optimize the cutting response. The integrated GRA–RSM–GA technique was appropriate for optimizing various machining issues.

Several studies examining SPRT performance were found. Therefore, the present study obtains the optimal cutting conditions of surface roughness during machining using the SPRT cutting tool. An experiment is conducted on the turning process of K110 which has many applications such as cutting tools, dies of deformation process, and tools in ceramic and plastic industry [15], [16]. The experimental carried out under various cutting conditions, such as cutting velocity ($v_c$), feed rate (f), depth of cut ($a_p$), and constant inclination angle.

The CCD-based study approach examines how cutting conditions affect surface roughness ($R_a$) to determine the optimal cutting parameter. Analysis of variance (ANOVA) and a second-order regression model were developed. To improve the SPRT cutting condition, GA was used. In order to further optimize $R_a$ and the associated cutting conditions assessed using GA, hybrid CCD-GA was developed.

# 2 EXPERIMENTAL WORK

## 2.1 Materials and Experimental Setup

Turning tests were performed on a central lathe (VEB Großdrehmaschinenbau 8. Mai, Karl-Marx-Stadt DLZ 450-1600 L+Z lathe) 10.3 kW spindle motor. The experiments were conducted using a tool holder of an SPRT under dry conditions (Figure 1). A tungsten carbide insert was used with a 6 mm thickness, 16 mm outer diameter, and 6.5 mm inner diameter. The inserts had a 0° rake angle and a 100° clearance angle measured over the insert's circumference. The workpieces of machining tests are three cylindrical K110 steel bars of 40 mm diameter and 800 mm length. Before the experiments, the material hardness was determined using a portable Vickers tester (KRAUTKAMER), and all specimens were acceptable in the range of 232 $V_{10}$. The chemical composition of K110 steel was determined using SPECTROLAB, and Table 1 shows the results.

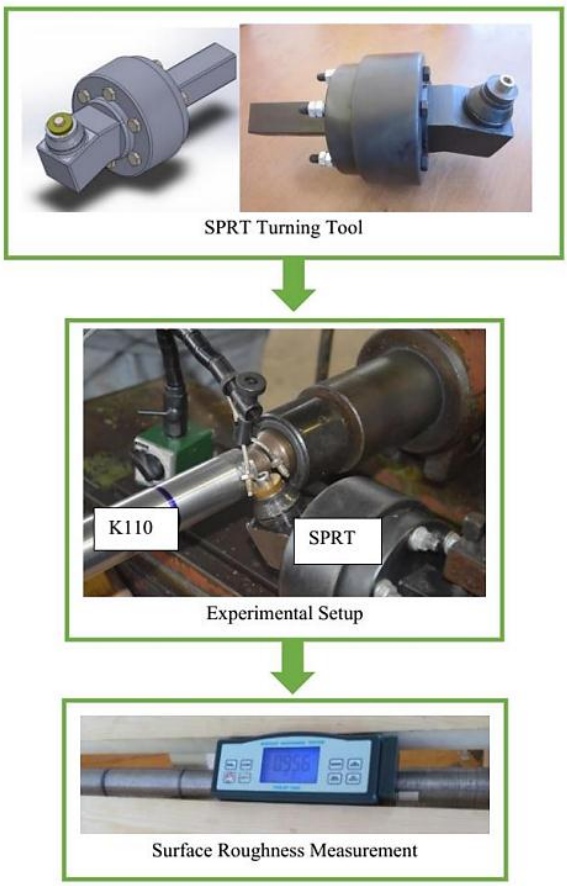


**Figure 1: Scheme of Experimental work**

**Table 1. K110 Steel Chemical Composition Results**

| Element | C% | Fe% | Mn% | P% |
|---|---|---|---|---|
| Weight% | 1.81 | 85.42 | 0.226 | 0.0243 |
| Element | S% | Cr% | Mo% | V% |
| Weight% | 0.00841 | 11.01 | 0.75 | 0.75 |

Surface roughness was measured using a surface roughness tester with a cutoff of 0.8 mm. A wooden fixture (Figure 1) fixed the device horizontally for accurate readings. Six readings occurred in each angle over six angles, resulting in 36 readings for each run. The mean value was then calculated. The accuracy of surface roughness values within range of ± 5% according to the measurement uncertainty.

### 2.2 Process Parameters and CCD

The most widespread turning parameters obtained by researchers are $v_c$ (m/min), f (mm/rev), and $a_p$ (mm). Surface roughness was used to determine the cutting performance for each set of turning parameters. In order to analyses three main parameters at three levels and model a second-order response surface, RSM was applied using CCD. To figure out the optimal parameter, the GA is used.

**Table 2. Rotatable central composite design levels of the cutting parameters.**

| Parameters | Coded levels | | |
|---|---|---|---|
| | -1 | 0 | 1 |
| $v_c$ (m/min) | 70 | 105 | 140 |
| f (mm/rev) | 0.04 | 0.1 | 0.16 |
| $a_p$ (mm) | 0.1 | 0.2 | 0.3 |

**Table 3. Design of experiment.**

| Run | $v_c$ (m/min) | f (mm/rev) | $a_p$ (mm) | $R_a$ (µm) |
|---|---|---|---|---|
| 1 | 46.14 | 0.1 | 0.2 | 1.02 |
| 2 | 140 | 0.16 | 0.1 | 1.1 |
| 3 | 105 | 0.2 | 0.2 | 0.66 |
| 4 | 163.86 | 0.1 | 0.2 | 0.71 |
| 5 | 70 | 0.04 | 0.3 | 1.1 |
| 6 | 105 | 0.1 | 0.03 | 1.43 |
| 7 | 70 | 0.16 | 0.1 | 1.25 |
| 8 | 70 | 0.04 | 0.1 | 0.87 |
| 9 | 140 | 0.04 | 0.3 | 0.81 |
| 10 | 140 | 0.16 | 0.3 | 0.92 |
| 11 | 70 | 0.16 | 0.3 | 1.11 |
| 12 | 105 | 0.001 | 0.2 | 0.89 |
| 13 | 140 | 0.04 | 0.1 | 0.58 |
| 14 | 105 | 0.1 | 0.37 | 1.56 |
| 15 | 105 | 0.1 | 0.2 | 1.31 |
| 16 | 105 | 0.1 | 0.2 | 1.35 |
| 17 | 105 | 0.1 | 0.2 | 1.36 |
| 18 | 105 | 0.1 | 0.2 | 1.36 |
| 19 | 105 | 0.1 | 0.2 | 1.37 |
| 20 | 105 | 0.1 | 0.2 | 1.37 |

Three trials were needed for the rotatable CCD: $2^k$ factorial, $2k$ axial, and $n$ center point trials, where $k$ specifies the number of components explored in the experiment [17], [18]. Eight factorial trials, six axial trials, and six center point trials (in total 20) were considered. The rotatability value $\alpha$, referring to the uniformity of prediction error, is computed as $[(2^k)^{1/4}]$, 1.682. Table 2 and Table 3 show the cutting parameters and their levels and the surface roughness results of experiments based on the rotatable CCD, respectively.

### 2.3 Regression Modelling

RSM analyzes the influence of independent variables (cutting parameters) on a specific quality characteristic called response ($R_a$) [19]. The relationship between the measured responses and cutting settings is provided by Equation (1).

$$Y = \Psi(\mathrm{vc}, f, d) + \epsilon, \quad (1)$$

where Y is the output response (surface roughness) and ε is the random error distributed about response Y. For the response of $R_a$, the regression technique was utilised to create polynomial (second-order) mathematical models [20] (Equation (2)).

$$Y = \beta_0 + \beta_1 v_c + \beta_2 f + \beta_3 a_p + \beta_4 v_c f + \beta_5 v_c a_p + \beta_6 f a_p + \beta_7 v_c^2 + \beta_8 f^2 + \beta_9 a_p^2 \quad (2)$$

In Equation (3), $R_a$ is the predicted surface roughness for the machining process. $R^2$ was 0.9891, and adjusted $R^2$ was 0.9792.

$$R_a = -0.833 + 0.02329 v_c + 20.60 f - 0.406 a_p - 0.000131 v_c^2 - 84.12 f^2 + 6.11 a_p^2 + 0.01429 v_c f - 0.00143 v_c a_p - 16.25 f a_p \quad (3)$$

## 3 GENETIC ALOGRITHM

In science and engineering, GAs have been employed as intelligent and heuristic tools for addressing real optimization issues cost-effectively. The GA generates a population of candidate solutions as well as a random number of generations in individuals. Traditionally, only a single point is generated and the next point is chosen using a deterministic rule. Each generation assesses individual fitness functions. The GA employs criteria to establish a fitness function's global minimum value [20][21].

## 4 RESULT AND DESCUSSION

### 4.1 ANOVA Results for Response

ANOVA is used to examine independent parameters, such as $v_c$, f, and $a_p$, and determine which ones significantly affect performance parameters ($R_a$) [22]. MINITAB 19 statistical software was used for analyses. Table 4 shows the ANOVA results for surface roughness ($R_a$).

The ANOVA in Table 4 shows the individual model coefficient's interaction and square terms and corresponding *P*-value. When the relationship between $R_a$ and cutting parameters is present, the *P*-value is <0.05, indicating that the regression model is satisfactory at a 95% confidence level. The F-value is the ratio of variation resulting from the error term to variance resulting from individual components. F > 4 indicates

that altering the cutting parameter significantly affects the $R_a$. [23]. Cutting velocity ($v_c$ ) has the greatest impact on $R_a$, followed by feed rate ($f$) and depth of cut ($a_p$).

**Table 4. ANOVA results for $R_a$**

| Source | DF | Sum of Square | Mean Squares | F-Value | P-Value |
|---|---|---|---|---|---|
| Regression | 9 | 1.54871 | 0.172079 | 100.39 | 0.000 |
| Linear | 3 | 0.16836 | 0.056120 | 32.74 | 0.000 |
| $v_c$ | 1 | 0.10479 | 0.104787 | 61.13 | 0.000 |
| f | 1 | 0.06311 | 0.063112 | 36.82 | 0.000 |
| $a_p$ | 1 | 0.00046 | 0.000459 | 0.27 | 0.616 |
| Square | 3 | 1.28306 | 0.427688 | 249.50 | 0.000 |
| $v_c$ * $v_c$ | 1 | 0.37229 | 0.372286 | 217.18 | 0.000 |
| f*f | 1 | 0.81506 | 0.815056 | 475.48 | 0.000 |
| $a_p$ * $a_p$ | 1 | 0.05614 | 0.056142 | 32.75 | 0.000 |
| 2-Way Interaction | 3 | 0.08345 | 0.027817 | 16.23 | 0.000 |
| $v_c$ *f | 1 | 0.00720 | 0.007200 | 4.20 | 0.068 |
| $v_c$ * $a_p$ | 1 | 0.00020 | 0.000200 | 0.12 | 0.740 |
| f * $a_p$ | 1 | 0.07605 | 0.076050 | 44.37 | 0.000 |
| Error (Residual) | 10 | 0.01714 | 0.001714 | | |
| Lack-of-Fit | 5 | 0.01461 | 0.002922 | 5.77 | 0.039 |
| Pure Error | 5 | 0.00253 | 0.000507 | | |
| Total | 19 | 1.56586 | | | |
| St deviation | $R^2$ | Adjusted $R^2$ | Predicted $R^2$ | | |
| 0.0414026 | 98.91% | 97.92% | 91.96% | | |

For determining the coefficient, the adjusted $R^2$ value of 0.9792 is close to predicted value of 0.9196. The models developed during the experimental analysis are statistically significant, as shown by the regression coefficient ($R^2 > 0.9891$).

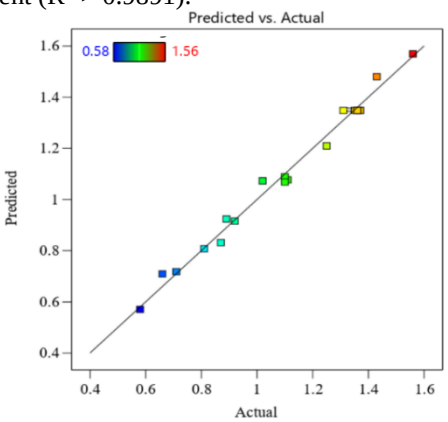


**Figure 2: Predicted and actual value of surface roughness**

Figure 2 compares the experimental data to the expected values calculated using the regression mathematical model over 20 runs. It demonstrates that most predicted results are extremely close to the actual experimental results, with a slight deviation between expected and real values. Furthermore, it indicates that the regression model is effective and useful for predicting the optimization cutting parameters for best surface roughness.

The interaction of cutting parameters in three-dimensions as it relates to $R_a$ is shown in Figure 3. While creating interaction surface plots between two parameters, one parameter is kept constant. During the interaction between $v_c$ and f, the $a_p$ is marked as 0.1 mm. Additionally, when the $v_c$ and $a_p$ interact, the f is marked as 0.04 mm/rev. Finally, the interaction between the f and $a_p$ is presented at a $v_c$ of 140 m/min.

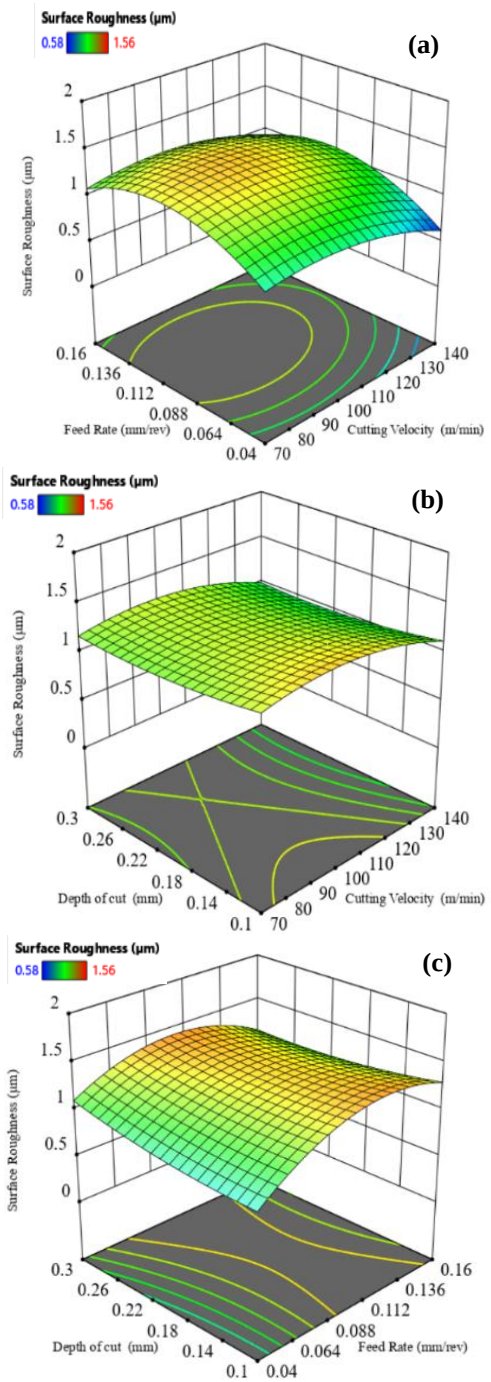


**Figure 3: Ra 's three-dimensional plots with $v_c$ and f in (a), $v_c$ and $a_p$ in (b), and f and $a_p$ in (c).**

The $v_c$ significantly affects the resulting $R_a$ (Figure3 (a)). The increase in $v_c$ decreased the $R_a$ at a $v_c$

from 70 to 140 m/min. The decrease in the f minimizes the $R_a$ validated with turning K110 using single point cutting tool [15].

Figure 3 (b) shows a three-dimensional interaction plot of $v_c$ and $a_p$. The decrease in $a_p$, thus, the generated $R_a$ of the turning process, has a slight significant effect, verified by ANOVA. Finally, Figure 3 (c) shows the three-dimensional interaction plot between f and $a_p$. The plot indicates that the increase in the f and $a_p$ will increase the $R_a$. The best $R_a$ will be obtained at the lowest f and $a_p$ [13].

### 4.2 GA Results

The best combination of SPRT independent variables that contribute to the minimal possible of surface roughness is found in the last stage using GA. Using the GA, the turning boundary condition, $v_c$, f, and $a_p$ are subjected to the objective function of minimizing the $R_a$ suggested in Equation (3),

Minimize $R_a$ ($v_c$, $f$, $a_p$)

Subjected to ranges of cutting conditions

$70 \leq v_c \leq 140$

$0.04 \leq f \leq 0.16$

$0.1 \leq a_p \leq 0.3$

The fitness value and run solver performance statistics from MATLAB indicate the best $R_a$ and corresponding cutting parameters for the GA optimization technique.

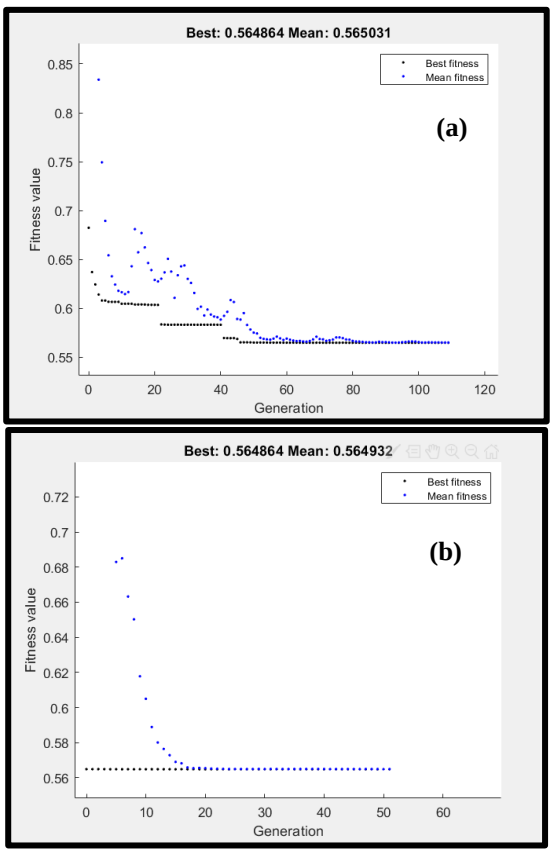


**Figure 4: Optimum surface roughness by (a) Pure Genetic and (b) Hybrid CCD-GA**

At 140 m/min, 0.04 mm/rev, and 0.103 mm for $v_c$, f, and $a_p$, respectively, the best $R_a$ value by GA is 0.564 µm (Figure 4 (a)). The $R_a$ values of CCD compared with the GA technique are 0.58 and 0.564 µm, respectively.

A hybrid CCD-GA was done to enhance the GA performance. Based on CCD optimum cutting parameters of $v_c$, f, and $a_p$, the initial population of hybrid CCD-GA is 140 m/min, 0.04 mm/rev, and 0.1 mm, respectively. The optimum generated $R_a$ using the hybrid CCD-GA is 0.564 µm (Figure 4 (b)), better than $R_a$ using CCD.

**Table 5. Summary of optimum result and their cutting condition**

| | Optimum Cutting Condition | | | $R_a$ |
|---|---|---|---|---|
| | $v_c$ | f | $a_p$ | |
| CCD | 140 | 0.04 | 0.1 | 0.58 |
| GA | 140 | 0.04 | 0.103 | 0.564 |
| CCD-GA | 140 | 0.04 | 0.103 | 0.564 |

For the GA optimization technique, the surface roughness values of CCD, GA, and hybrid CCD-GA are 0.58, 0.564, and 0.564 µm, respectively (Table 5).

## 5 CONCLUSION

This paper investigates applying the parameter design CCD in selecting the optimum cutting parameters for machining hard steel K110 using SPRT. Based on the experimental and optimization outcomes, the following conclusions can be drawn.

- The experimental investigation's models were developed using the CCD technique, which produced a strong regression coefficient ($R^2$ > 0.9891) and forecasted $R^2$ = 91.96 %.
- ANOVA reveals that $v_c$ has the most impact on $R_a$, followed by f and $a_p$.
- The minimum $R_a$ value was 0.58 µm at 140 m/min of $v_c$, 0.04 mm/rev of $f$, and 0.3 mm of $a_p$.
- The confirmatory test revealed that the expected and observed values correlate well.
- The GA recommends that the minimum $R_a$ is 0.564 µm and the corresponding cutting variable values are 140 m/min, 0.04 mm/rev, and 0.103 mm for $v_c$, f, and $a_p$, respectively.
- The hybrid CCD-GA has a minimum $R_a$ of 0.564 µm compared with the CCD minimum $R_a$ of 0.58 µm.

**Acknowledgments**

The authors would like to extend their thanks and gratitude to the technicians in the workshop of the Faculty of Engineering, Port Said University – Egypt

**Credit Authorship Contribution Statement**

**H. Kouta**: Methodology, Formal analysis, Software, Data Curation, Writing, Review & Editing.

**S. Elsanabary**: Experimental investigation, Resources, Formal analysis, Writing-original draft, Review & Editing.

**Declaration of Competing Interest**

The authors declare that they have no known competing financial interests or personal relationships that could have appeared to influence the work reported in this paper.

**Conflicts of Interest**

The authors declare that there is no conflict of interest regarding the publication of this paper

## 6 REFERENCES


[1] W. Ahmed, H. Hegab, A. Mohany, and H. Kishawy, "On machining hardened steel AISI 4140 with self-propelled rotary tools: experimental investigation and analysis," The International Journal of Advanced Manufacturing Technology, vol. 113, no. 11, pp. 3163–3176, 2021.

[2] W. Ahmed, H. Hegab, A. Mohany, and H. Kishawy, "Analysis and Optimization of Machining Hardened Steel AISI 4140 with Self-Propelled Rotary Tools," Materials, vol. 14, no. 20, p. 6106, 2021.

[3] M. Kotb, A. Barakat, A. Mahrous, and A. Elkaseer, "Thermal Behavior of Self-Propelled Rotary Tool in Machining AISI 4140 Hardened Steel," Engineering Research Journal, vol. 1, no. 47, pp. 82–89, 2021.

[4] R. Teimouri, S. Amini, and N. Mohagheghian, "Experimental study and empirical analysis on effect of ultrasonic vibration during rotary turning of aluminum 7075 aerospace alloy," Journal of Manufacturing Processes, vol. 26, pp. 1–12, 2017.

[5] S. Wojciechowski, R. W. Maruda, G. M. Krolczyk, and P. Niesłony, "Application of signal to noise ratio and grey relational analysis to minimize forces and vibrations during precise ball end milling," Precision Engineering, vol. 51, pp. 582–596, 2018.

[6] A. Hosokawa, T. Ueda, R. Onishi, R. Tanaka, and T. Furumoto, "Turning of difficult-to-machine materials with actively driven rotary tool," CIRP annals, vol. 59, no. 1, pp. 89–92, 2010.

[7] P. Nieslony et al., "Study on physical and technological effects of precise turning with self-propelled rotary tool," Precision Engineering, vol. 66, pp. 62–75, 2020.

[8] U. Olgun and E. Budak, "Machining of difficult-to-cut-alloys using rotary turning tools," Procedia CIRP, vol. 8, pp. 81–87, 2013.

[9] H. A. Kishawy, L. Pang, and M. Balazinski, "Modeling of tool wear during hard turning with self-propelled rotary tools," International Journal of Mechanical Sciences, vol. 53, no. 11, pp. 1015–1021, 2011.

[10] J. Kossakowska and K. Jemielniak, "Application of Self-Propelled Rotary Tools for turning of difficult-to-machine materials," Procedia CIRP, vol. 1, pp. 425–430, 2012.

[11] N. Suzuki et al., "Force prediction in cutting operations with self-propelled rotary tools considering bearing friction," Procedia CIRP, vol. 14, pp. 125–129, 2014.

[12] M. Ghaedi, F. N. Azad, K. Dashtian, S. Hajati, A. Goudarzi, and M. Soylak, "Central composite design and genetic algorithm applied for the optimization of ultrasonic-assisted removal of malachite green by ZnO Nanorod-loaded activated carbon," Spectrochimica Acta Part A: Molecular and Biomolecular Spectroscopy, vol. 167, pp. 157–164, 2016.

[13] T. B. Rao, A. G. Krishna, R. K. Katta, and K. R. Krishna, "Modeling and multi-response optimization of machining performance while turning hardened steel with self-propelled rotary tool," Advances in Manufacturing, vol. 3, no. 1, pp. 84–95, 2015.

[14] T. B. Rao and N. Baki, "An evolutionary-based hybrid approach for simultaneous optimisation of multiple responses in self-propelled rotary turning process," International Journal of Manufacturing Research, vol. 14, no. 1, pp. 82–99, 2019.

[15] A. D. Jewlikar, V. V Joshi, and S. Borse, "HPT Process Parameter Optimization in Dry Turning of Bohler K110 Steel," Materials Today: Proceedings, vol. 2, no. 4–5, pp. 2414–2422, 2015.

[16] N. Annamalai, V. Sivaramakrishnan, and N. Baskar, "Modeling of Cold Work Tool Steel–Bohler K110 for Enhancing Production and Quality Characteristics in Electric Discharge Machining," International Journal of Applied Engineering Research, vol. 10, no. 76, p. 2015.

[17] B. Ait-Amir, P. Pougnet, and A. El Hami, "Meta-model development," in Embedded mechatronic systems 2, Elsevier, 2020, pp. 157–187.

[18] S. K. Behera, H. Meena, S. Chakraborty, and B. C. Meikap, "Application of response surface methodology (RSM) for optimization of leaching parameters for ash reduction from low-grade coal," International Journal of Mining Science and Technology, vol. 28, no. 4, pp. 621–629, 2018.

[19] A. Asghar, A. A. Abdul Raman, and W. M. A. W. Daud, "A comparison of central composite design and Taguchi method for optimizing Fenton process," The Scientific World Journal, vol. 2014, 2014.

[20] A. J. Santhosh, A. D. Tura, I. T. Jiregna, W. F. Gemechu, N. Ashok, and M. Ponnusamy, "Optimization of CNC turning parameters using face centred CCD approach in RSM and ANN-genetic algorithm for AISI 4340 alloy steel," Results in Engineering, vol. 11, p. 100251, 2021.

[21] A. Dadrasi, S. Fooladpanjeh, and A. A. Gharahbagh, "Interactions between HA/GO/epoxy resin nanocomposites: optimization, modeling and mechanical performance using central composite design and genetic algorithm," Journal of the Brazilian Society of Mechanical Sciences and Engineering, vol. 41, no. 2, p. 63, 2019.

[22] S. Elsanabary and H. K. Kouta, "Optimization of Inertia Friction Welding of Dissimilar Polymeric PA6-PVC Hollow Cylinders by Genetic Algorithm," Port-Said Engineering Research Journal, vol. 25, no. 1, pp. 91–100, 2021.

[23] W. H. P. Yang and Y. S. Tarng, "Design optimization of cutting parameters for turning operations based on the Taguchi method," Journal of materials processing technology, vol. 84, no. 1–3, pp. 122–129, 1998.